JLB

Article

Myosin-IIA regulates leukemia engraftment and brain infiltration in a mouse model of acute lymphoblastic leukemia

Eric J. Wigton,[,1,2] Scott B. Thompson,*[,†,1] Robert A. Long,* and Jordan Jacobelli*[,†,3]*

*Department of Biomedical Research, National Jewish Health, Denver, Colorado, USA; and †Department of Immunology and Microbiology, University of Colorado School of Medicine, Denver, Colorado, USA

RECEIVED AUGUST 5, 2015; REVISED DECEMBER 31, 2015; ACCEPTED JANUARY 4, 2016. DOI: 10.1189/jlb.1A0815-342R

ABSTRACT

Leukemia dissemination (the spread of leukemia cells from the bone marrow) and relapse are associated with poor prognosis. Often, relapse occurs in peripheral organs, such as the CNS, which acts as a sanctuary site for leukemia cells to escape anti-cancer treatments. Similar to normal leukocyte migration, leukemia dissemination entails migration of cells from the blood circulation into tissues by extravasation. To extravasate, leukemia cells cross through vascular endothelial walls via a process called transendothelial migration, which requires cytoskeletal remodeling. However, the specific molecular players in leukemia extravasation are not fully known. We examined the role of myosin-IIA a cytoskeletal class II myosin motor protein, in leukemia progression and dissemination into the CNS by use of a mouse model of Bcr-Abl-driven B cell acute lymphoblastic leukemia. Small hairpin RNA-mediated depletion of myosin-IIA did not affect apoptosis or the growth rate of B cell acute lymphoblastic leukemia cells. However, in an in vivo leukemia transfer model, myosin-IIA depletion slowed leukemia progression and prolonged survival, in part, by reducing the ability of B cell acute lymphoblastic leukemia cells to engraft efficiently. Finally, myosin-IIA inhibition, either by small hairpin RNA depletion or chemical inhibition by blebbistatin, drastically reduced CNS infiltration of leukemia cells. The effects on leukemia cell entry into tissues were mostly a result of the requirement for myosin-IIA to enable leukemia cells to complete the transendothelial migration process during extravasation. Overall, our data implicate myosin-IIA as a key mediator of leukemia cell migration, making it a promising target to inhibit leukemia dissemination in vivo and potentially reduce leukemia relapses.
***J. Leukoc. Biol.* 100: 143–153; 2016.**

Abbreviations: 7-AAD = 7-aminoactinomycin D, ALL = acute lymphoblastic leukemia, APC = allophycocyanin, B-ALL = B cell acute lymphoblastic leukemia, KD = knockdown, MyoIIA/B/C = myosin-II A/B/C, PacBlue = Pacific Blue, shRNA = small hairpin RNA, TEM = transendothelial migration, TKI = tyrosine kinase inhibitor

The online version of this paper, found at www.jleukbio.org, includes supplemental information.

Introduction

ALL is the most common type of pediatric cancer, and the B cell precursor ALL is the most common subtype [1]. Whereas current treatments that use combinations of TKIs, radiation, and bone marrow transplants can achieve initial remission, relapse rates remain significant. Dissemination of leukemia—the infiltration of leukemia cells into tissues outside of the bone marrow—carries a poor prognosis and can play a role in relapse. Relapsing leukemia often occurs in the "sanctuary" of the CNS, where the reduced permeability of the blood-brain barrier can protect leukemia cells from chemotherapy and TKIs [2–5]. Current approaches for preventing or treating CNS-relapsing leukemia can involve particularly severe treatments, such as cranial irradiation and intrathecal chemotherapy, and survival rates among children with relapsed ALL remain low [6, 7]. Novel therapeutics that inhibit leukemia dissemination into the CNS could provide useful cotherapies to prevent relapse and increase the long-term survival of patients.

Dissemination into tissues requires that leukemia cells leave the blood circulation by extravasation. Following selectin-mediated rolling [8], lymphocytes adhere to endothelial vascular walls by chemokine and integrin-mediated adhesion to the endothelium [9]. Subsequently, lymphocytes cross the endothelial barrier via a process known as TEM [10, 11]. To initiate TEM, a lymphocyte must crawl along the endothelial cell barrier to find a permissive site and then squeeze between endothelial cells to complete the process [10, 11]. The morphologic changes and mechanical force required to cross the endothelial barrier rely on remodeling of the cytoskeleton and the function of cellular motor proteins [11, 12]. Previous studies have indicated that the mechanisms of lymphocyte and leukemia and lymphoma cell extravasation may be similar, making cytoskeletal effector proteins attractive potential therapeutic targets for preventing leukemia dissemination [13, 14]. However, the cytoskeletal molecular players regulating leukemia cell extravasation and dissemination are mostly unknown.

1. These authors contributed equally to this work.
2. Current affiliation: University of California San Francisco, California, USA.
3. Correspondence: National Jewish Health, 1400 Jackson St., Denver, CO 80206, USA. E-mail: jacobellij@njhealth.org

We have recently identified MyoIIA, a cytoskeletal class II nonmuscle myosin motor protein, as being important for T cell extravasation [15, 16]. MyoIIA is also required for activated T cell entry into the CNS [15]. Therefore, we investigated if MyoIIA played a role in lymphoid leukemia extravasation and dissemination, including infiltration into the CNS.

MyoIIA functions by cross-linking actin filaments, and through its motor activity, it contracts the local actin cytoskeleton to generate mechanical force. Force generation by MyoIIA promotes a number of cellular functions, including cytokinesis, cell polarity, cell adhesion, and cell migration [12, 17, 18]. Regarding cell migration, MyoIIA is important for motility within tissues, where it can provide the force necessary to detach intercellular and extracellular matrix adhesions [16, 19], and MyoIIA facilitates lymphocyte extravasation by providing the force necessary to squeeze the rigid nucleus through restrictive barriers [15, 20]. MyoIIA has also been implicated in promoting the invasiveness of cancers, such as gliomas and carcinomas [21–24]. In the context of leukemia, it has been shown that MyoIIA promotes in vitro motility of leukemia cells [25, 26]. However, the role of MyoIIA in leukemia cell extravasation and dissemination in vivo had yet to be examined.

Here, we use shRNA-mediated KD, as well as chemical inhibition of MyoIIA in Bcr-Abl$^+$ pre-B-ALL cells to investigate its role in leukemia progression, dissemination, and extravasation. We show that depletion of MyoIIA in B-ALL cells prolongs recipient mouse survival and impairs leukemia engraftment in vivo. MyoIIA inhibition also reduces the ability of leukemia cells to infiltrate the CNS. Furthermore, our data show that leukemia cells require MyoIIA for migration in response to chemokine and for efficient completion of TEM across brain-derived endothelial cells. Overall, our data identify MyoIIA as a key regulator of B-ALL cell migration and extravasation and suggest that MyoIIA could be a potential therapeutic target to prevent leukemia dissemination.

MATERIALS AND METHODS

B-ALL cells and shRNA transduction

Arf $^{-/-}$ BCR-Abl$^+$ B-ALL cells were originally made by Charles Sherr and colleagues [27] (St. Jude Children's Research Hospital, Memphis, TN, USA) and donated by James DeGregori (University of Colorado School of Medicine, Denver, CO, USA). Original luciferase$^+$ B-ALL cells were retrovirally transduced using the pSIREN-RetroQ-ZsGreen1 vector (Clontech Laboratories, Mountain View, CA, USA) to express the MyoIIA-specific shRNA (MyoIIA KD B-ALL) sequence TCCGACTGTAAACCGTCTCAA (targeting position 6592 of the MyoIIA mRNA based on sequence NM_022410.1 [28]) or sequence CGGTAAATTCATTCGTATCAA (targeting position 867 of the MyoIIA mRNA based on sequence NM_022410.1) or alternatively, a control, nonsilencing shRNA (control B-ALL, sequence TCTATAGAACCCTCAATAT), as well as the fluorescent protein ZsGreen. The transduced ZsGreen$^+$ B-ALL cells were sorted and used immediately for experiments or cryogenically frozen for later use. B-ALL cells used for experiments were cultured in vitro for no more than 6 wk, and MyoIIA KD was routinely monitored by Western blot to be at least 80% for shRNA-6592 or 70% for shRNA-867 compared with control cells.

Western blot

Nonmuscle class II myosin protein isoform levels in cell lysates were assessed by Western blot using anti-MyoIIA rabbit polyclonal antibody (Cell Signaling Technology, Beverly, MA, USA), anti-MyoIIB rabbit mAb (clone D8H8; Cell Signaling Technology), or anti-MyoIIC rabbit polyclonal antibody (Covance/BioLegend, San Diego, CA, USA). Mouse anti-tubulin (Sigma-Aldrich, St. Louis, MO, USA) was used as a loading control. Primary antibody staining on membrane blots was detected using IRDye 680- and/or IRDye 800-conjugated secondary antibodies (LI-COR Biosciences, Lincoln, NE, USA) and analyzed on an Odyssey near-infrared imaging system (LI-COR Biosciences). COS7 and PC12 cell lysates (ECM Biosciences, Versailles, KY, USA) were used as positive controls for MyoIIB and MyoIIC blotting.

In vitro B-ALL proliferation

B-ALL cells were grown in RPMI 1640 (Mediatech/Corning, Corning, NY, USA), with 10% FBS (Hyclone, GE Healthcare Life Sciences, Logan, UT, USA), 5 μM 2-ME, penicillin, streptomycin, and L-glutamine (all from Life Technologies, Thermo Fisher Scientific, Waltham, MA, USA). B-ALL cells were initially set to a concentration of 2.5×10^5/ml and diluted every 2 d by a 1:10 factor. Cell counts were taken by hemocytometer in the presence of Trypan blue (Sigma-Aldrich) to exclude dead cells. The B-ALL cells were cultured for up to 10 d, and growth curves were generated by calculating the cell numbers over the entire growth period.

Apoptosis assay

B-ALL cells were cultured for 48 h at 37°C and then stained with APC-Annexin V and 7-AAD (both from BD PharMingen, San Diego, CA, USA). Stained cells were then analyzed by flow cytometry using a CyAn ADP (Beckman Coulter, Brea, CA, USA), and apoptotic cells were quantified based on the Annexin V-positive population.

Leukemia in vivo survival assays

For leukemia survival assays, we used a B-ALL transfer model, in which 5×10^4 control or MyoIIA KD B-ALL cells/mouse were adoptively transferred by tail-vein injection into cohorts of 5 C57BL/6 CD45.1$^+$, 6- to 10-wk-old age-matched male mice (Charles River Laboratories, Wilmington, MA, USA). All experiments involving mice were approved by the Institutional Animal Care and Use Committee at National Jewish Health, and all efforts were made to minimize mouse suffering. Recipient mice were monitored daily, and animals showing signs of morbidity (hunched position, lethargy, ruffled fur) and/or >15% loss in starting body weight (taken 6 d post-transfer) were scored as having leukemia and euthanized for humane reasons.

Leukemia progression analysis

For time-course leukemia progression experiments, 5×10^4 control or MyoIIA KD B-ALL cells were transferred into age-matched, 8- to 12-wk-old C57BL/6 CD45.1$^+$ recipient male mice, and then, every 3 d post-transfer, recipient mice were randomly selected for analysis. For intravascular labeling of B-ALL cells, recipient mice were intravenously injected with 3 μg anti-CD19-APC (clone 6D5; BioLegend), 4 min before CO_2 euthanasia. After euthanasia, blood was then harvested by cardiocentesis, and mice were subsequently perfused with saline to eliminate residual blood in vessels within tissues. Spleen and bone marrow were harvested and mechanically processed to a single-cell suspension. RBCs in the spleen and blood were lysed using 175 mM ammonium chloride (Sigma-Aldrich) for 5 min. The liver was harvested and digested by collagenase D (4000 Mandl U/ml; Roche Diagnostics, Indianapolis, IN, USA) and DNase I (25 μg/ml; Roche Diagnostics) for 30 min. Lymphocytes from liver samples were isolated using Histopaque 1119 (Sigma-Aldrich). The samples were then stained with anti-CD45.1 PacBlue (clone A20; BioLegend) and acquired on a CyAn ADP flow cytometer. The transferred B-ALL cells were identified as ZsGreen$^+$ CD45.1$^-$ cells, with B-ALL cells still remaining in the vasculature also CD19$^+$, and cells having infiltrated tissues being CD19$^-$.

Leukemia engraftment experiments

For these short-term transfer experiments, B-ALL cells were labeled for 15 min at 37°C in HBSS (Mediatech/Corning) with 1 μM Violet Proliferation Dye 450 (BD Biosciences, San Jose, CA, USA) or 5 μM eFluor 670 cell proliferation dye

(eBioscience, San Diego, CA, USA). To avoid potential artifacts from dye labeling, the 2 dyes were switched between experimental repeats. Dye-labeled control and MyoIIA KD B-ALL cells (2.5×10^6 each) were cotransferred by tail-vein injection into 8- to 16-wk-old C57BL/6 CD45.1$^+$ male mice; 8 or 24 h later, recipient mice were euthanized, and immediately following euthanasia, blood was harvested by cardiocentesis, and mice were subsequently perfused with saline to eliminate residual blood in vessels within tissues. Blood, spleen, and bone marrow were harvested and processed as described above in Leukemia progression analysis. The samples were then acquired on a CyAn ADP flow cytometer. The transferred B-ALL cells were identified as ZsGreen$^+$ cells, and control versus MyoIIA KD cells were distinguished based on their dye label.

Leukemia brain infiltration assay

Control or MyoIIA KD B-ALL cells (2×10^7 each) were transferred into age-matched, 8- to 12-wk-old C57BL/6 CD45.1$^+$ male mice. Eighteen hours later, intravascular B-ALL cells were labeled using a CD19-APC antibody, as described above in the Leukemia progression analysis, and following euthanasia, blood was harvested, and mice were perfused with saline. The brain was then harvested and mechanically processed to a single-cell suspension. Lymphocytes from brain samples were isolated using a 70%/30% Percoll gradient (Sigma-Aldrich). The samples were then stained with anti-CD45.1 PacBlue and acquired on a CyAn ADP flow cytometer. The transferred B-ALL cells were identified as ZsGreen$^+$ CD45.1$^-$ cells, with B-ALL cells remaining adhered inside the brain vasculature also CD19$^+$, and B-ALL cells having infiltrated the brain parenchyma being CD19$^-$. In similar experiments, we also tested the efficacy of blebbistatin in inhibiting MyoIIA and B-ALL cell entry into the brain. For these experiments, age-matched, 8- to 12-wk-old C57BL/6 CD45.1$^+$ male mice were treated with a single intravenous injection of vehicle only or (−)blebbistatin (the active enantiomer; Selleckchem.com, Houston, TX, USA) at 2.5 mg/kg, diluted in a 5% DMSO, 95% polyethylene glycol 400 solution (both from Sigma-Aldrich). One hour later, 2×10^7 control B-ALL cells were transferred into vehicle and blebbistatin-treated recipient mice. Twenty-four hours after transfer, intravascular B-ALL cells were labeled using a CD19-APC antibody, and following euthanasia, blood and brain were harvested, processed, and analyzed as just described. This short-term blebbistatin treatment was well tolerated and did not result in discernible toxic or adverse effects in the recipient mice.

Transwell migration assay

Twenty-four-well plate Transwell chambers (Corning) with 5 μm pores were used to assess the chemotaxis response of B-ALL cells. Control B-ALL cells, MyoIIA KD B-ALL cells, or control B-ALL cells (2×10^6 each) treated with 100 μM blebbistatin (±racemic mixture; EMD Millipore, Billerica, MA, USA) were added to the top of 5 μM Transwells. The bottom wells contained RPMI 1640 + 2% BSA (Sigma-Aldrich) + 10 mM HEPES (Life Technologies, Thermo Fisher Scientific), with or without 1 μg/ml CXCL12/stromal cell-derived factor 1α (PeproTech, Rocky Hill, NJ, USA) and with or without 100 μM blebbistatin. In addition, cells (4×10^5; 20% of cells added to Transwells) were placed directly into wells with no Transwell and used as a standard to calculate the percentage of migrated cells in the assay. The plate was incubated for 2 h at 37°C. Cells were then collected from the bottom wells and quantified using flow cytometry in the presence of flow cytometry cell-counting beads (Life Technologies, Thermo Fisher Scientific).

In vitro TEM under flow assay

Tissue culture-treated flow chambers (μ-Slide VI; ibidi, Madison, WI, USA) were seeded with bEnd.3 endothelial cells (American Type Culture Collection, Manassas, VA, USA), 48 h before the assay. The endothelial monolayers were treated with 40 ng/ml TNF-1α (PeproTech), 24 h before the assay, followed by 1 μg/ml CXCL12 and 1:100 anti-CD31/PECAM-1 APC (clone 390; BioLegend), 30–45 min before the assay. Staining for CD31 allowed us to visualize the membrane of the endothelial cells without perturbing the TEM process (data not shown and refs. [29, 30]). Control or MyoIIA KD B-ALL cells were resuspended at 2×10^6 cells/ml (in RPMI 1640 without Phenol red and with 2% BSA and 10 mM HEPES) and perfused onto the endothelial monolayer in the flow chamber at a shear flow of 0.25 dyne/cm^2 for 5 min. The flow rate was then raised to 2 dyne/cm^2 (physiologic shear flow) for the remainder of the imaging. Images were captured every 15 s over a 30-min time course using a Marianas spinning disk confocal microscope (equipped with a Yokogawa CSU-X1 spinning disk unit) with a 20× phase contrast objective and controlled with 3i SlideBook imaging software (3i, Intelligent Imaging Innovations, Denver, CO, USA). The microscope was equipped with an environmental control chamber set to 36.5°C. B-ALL cells were deemed to have undergone TEM, based on the disappearance of their phase-contrast ring using the same criteria as described previously [15]. The opening of endothelial junctions, visualized by CD31 staining underneath B-ALL cells, was used to determine TEM initiation by B-ALL cells.

Data analysis and statistics

Flow cytometry data were analyzed using FlowJo software (Version 9.5; TreeStar, Ashland, OR, USA). Prism software (GraphPad, La Jolla, CA, USA) was used to graph the data and calculate statistics. The statistical significance of data was determined by performing the Student's t test for single comparisons or ANOVA for multiple comparisons, followed by post hoc Tukey tests. For the Transwell chemotaxis assay, the leukemia in vitro proliferation, and the in vivo progression over time, 2-way ANOVA was used, followed by Bonferroni post-tests. Finally, in the case of survival curve data, the significance was determined using the log-rank (Mantel-Cox) test.

RESULTS

Depletion of MyoIIA does not affect leukemia cell viability and proliferation

As a leukemia model, we used an established mouse pre-B-ALL cell line obtained by transducing bone marrow cells from Arf$^{-/-}$ C57BL/6 mice with p185Bcr-Abl [27]. In this leukemia model, transferred Bcr-Abl$^+$ Arf$^{-/-}$ leukemogenic pre-B cells rapidly induce lymphoid leukemia in healthy, nonirradiated mice, with a high incidence of CNS infiltration [27, 31, 32]. To study the effects of MyoIIA on leukemia migration and dissemination, we used shRNAs to KD its expression. B-ALL cells were transduced with a retroviral vector coexpressing ZsGreen and MyoIIA-specifc or nonsilencing control shRNA constructs. For MyoIIA KD, we used a previously validated shRNA construct (targeting MyoIIA mRNA at position 6592) that we used successfully in primary mouse T cells [28], as well as a second MyoIIA-targeting shRNA sequence (targeting MyoIIA mRNA at position 867) to confirm further the specificity of this approach. After fluorescently sorting shRNA-transduced ZsGreen$^+$ B-ALL cells, MyoIIA shRNA 6592 consistently yielded cells with 80–90% KD of MyoIIA protein relative to control, shRNA-treated B-ALL cells (**Fig. 1A**), whereas MyoIIA shRNA 867 typically resulted in 70–80% MyoIIA KD (Supplemental Fig. 1A). As MyoIIA shRNA 6592 depleted MyoIIA to a greater extent, we used this shRNA for our experiments and validated our findings using shRNA 867 in select experiments.

Of the 3 class II nonmuscle myosin isoforms, mouse lymphocytes typically only express MyoIIA [33]. To confirm this expression pattern in B-ALL cells, we tested if MyoIIB and MyoIIC were aberrantly expressed in the B-ALL cells under steady-state conditions or as a compensatory mechanism in response to MyoIIA KD. With the use of Western blot analysis, we only detected trace amounts of MyoIIB and MyoIIC and did not

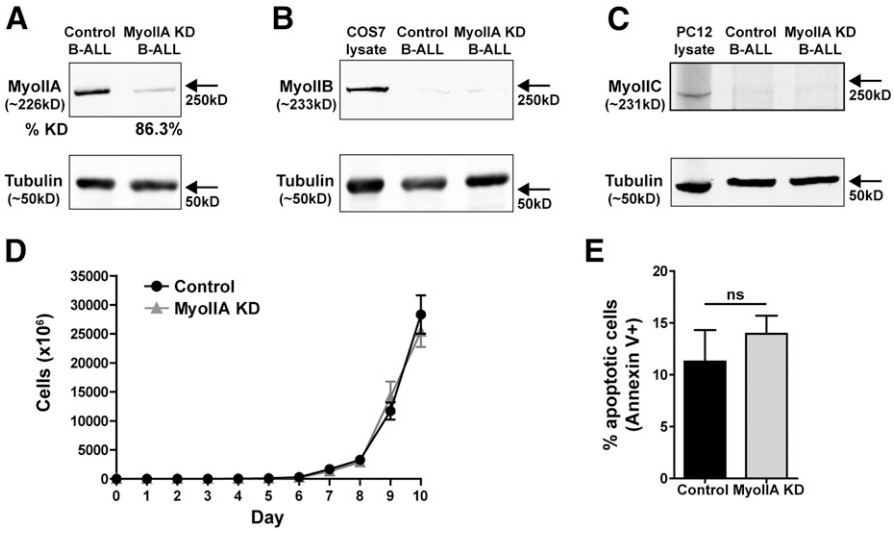

Figure 1. B-ALL cell proliferation and apoptosis are not altered by MyoIIA KD. B-ALL leukemia cells were transduced with retroviral vectors coexpressing control shRNA or MyoIIA-specific shRNA 6592 (MyoIIA KD) and ZsGreen. (A) Depletion of MyoIIA in ZsGreen$^+$-sorted MyoIIA KD cells compared with control shRNA-transduced cells was confirmed by densitometry analysis of Western blots stained with an isoform-specific MyoIIA antibody. Densitometry values were normalized to the relative protein loading measured by tubulin levels in each sample. Typical KD levels of MyoIIA were between 80% and 90%. (B and C) Expression of MyoIIB and MyoIIC in B-ALL leukemia cells. COS7 cells and PC12 cell lysates were used as positive controls for MyoIIB and MyoIIC expression, respectively. At most, only trace levels of MyoIIB and MyoIIC were detected by Western blot in B-ALL leukemia cells, and KD of MyoIIA did not result in increased expression of these other class II myosin isoforms. (D) MyoIIA KD B-ALL cells proliferate similarly to control B-ALL cells. In vitro growth curves of control and MyoIIA KD B-ALL leukemia cells. B-ALL cells were set at a concentration of 2.5×10^5/ml and diluted every 2 d by a 1:10 factor. The B-ALL cells were cultured for up to 10 d, and growth curves were generated from calculating total cell numbers over the entire growth period. (E) MyoIIA KD does not affect steady-state apoptosis of B-ALL cells. B-ALL leukemia cells were cultured for 48 h at 37°C and then stained with APC-Annexin V and 7-AAD. The percentage of apoptotic cells was determined by quantifying the Annexin V-positive population using flow cytometry. ns, Not significant. (A) Data are representative of at least 3 experiments. (B and C) Data are representative of 2 experiments. (D and E) Data are the means ± SEM averaged from at least 3 independent experiments.

see any up-regulation of these myosins following MyoIIA KD when compared with control shRNA B-ALL cells (Fig. 1B and C).

Given the reported role of MyoIIA in cytokinesis [34], we analyzed if depletion of MyoIIA altered the proliferation rate or apoptosis frequency of B-ALL cells. When comparing control and MyoIIA KD B-ALL cells, we did not observe significant proliferation differences over a 10-d period (Fig. 1D and Supplemental Fig. 1B). Likely, the residual MyoIIA was sufficient to allow B-ALL cells to divide normally. Furthermore, we did not detect significant differences in the apoptosis frequency of control vs. MyoIIA KD B-ALL cells when measured by Annexin V staining (Fig. 1E and Supplemental Fig. 1C).

MyoIIA depletion prolongs survival and slows leukemia progression

We then analyzed how MyoIIA affected B-ALL leukemia progression in vivo and if MyoIIA KD in leukemia cells resulted in prolonged survival in a leukemia transfer model. For these experiments, wild-type, immune-competent recipient mice were intravenously transferred with 5×10^4 control or MyoIIA KD B-ALL cells and monitored daily for leukemia incidence. This analysis revealed a significantly prolonged survival of the mice transferred with MyoIIA-deficient B-ALL cells (**Fig. 2A**). The median survival of control B-ALL recipient mice was 14 d, whereas the median survival of recipient mice transferred with MyoIIA KD B-ALL cells was 21.5 d. With the use of a second independent shRNA construct to target MyoIIA (shRNA 867), we confirmed that survival was significantly prolonged when transferring MyoIIA KD B-ALL cells as a result of MyoIIA depletion, rather than the result of possible off-target effects of the shRNAs (Supplemental Fig. 1D).

We next examined the effects of MyoIIA depletion on leukemia progression and dissemination over time. C57BL/6 recipient mice, expressing the congenic marker CD45.1$^+$, were transferred with 5×10^4 control or MyoIIA KD B-ALL cells (which express CD45.2). Leukemia progression in the recipient mice was monitored every 3 d by measuring the number of B-ALL cells in the blood, bone marrow, spleen, liver, and brain. We did not analyze leukemia progression beyond 9 d post-transfer, as control B-ALL recipient mice had reduced survival past this time point. The number of control or MyoIIA KD B-ALL cells was quantified by flow cytometry from single-cell suspensions of the harvested organs. B-ALL cells were identified by their expression of ZsGreen and CD45.2 (whereas endogenous leukocytes from the recipient mice were CD45.1$^+$). This ALL model is very aggressive, and we found a dramatic expansion of the B-ALL cells in all organs analyzed, particularly between d 6 and 9 post-transfer. When compared with control B-ALL cells, we observed a trend for reduced numbers of MyoIIA KD B-ALL cells over the time course in the bone marrow and spleen. This reduction in the number of MyoIIA KD B-ALL cells became statistically significant in all analyzed organs (blood, bone marrow, spleen, liver, and brain), 9 d post-transfer (Fig. 2B–F), which coincided with the major leukemia expansion. Overall, these data suggest that in the absence of MyoIIA leukemia progression, in vivo is slower.

Reduced engraftment of MyoIIA-deficient leukemia cells

As our data on MyoIIA KD B-ALL proliferation in vitro did not indicate a reduced growth rate of the MyoIIA-deficient cells (Fig. 1D), we investigated if differences in disease progression could be, at least in part, a result of reduced engraftment of the MyoIIA KD B-ALL cells. Therefore, we compared the ability of control and MyoIIA KD B-ALL cells to engraft within the bone marrow and spleen of recipient mice. For these experiments,

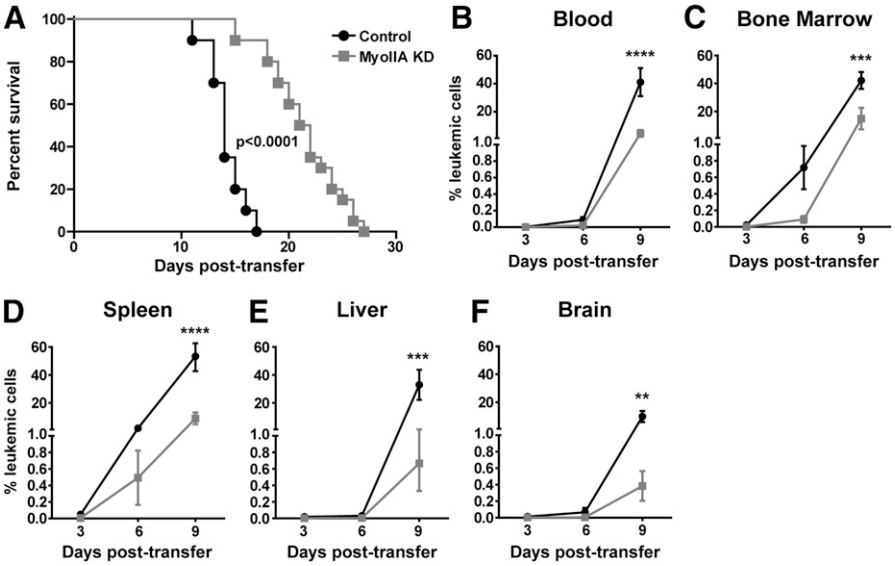

Figure 2. Depletion of MyoIIA in B-ALL cells prolongs survival and slows leukemia progression. C57BL/6 CD45.1$^+$ recipient mice were intravenously adoptively transferred with 5×10^4 ZsGreen$^+$ CD45.2$^+$ control (black circles) or MyoIIA KD (shRNA 6592; gray squares) B-ALL cells. (A) Depletion of MyoIIA in B-ALL cells results in prolonged survival of leukemia recipient mice. Recipient mice were monitored daily for signs of leukemia progression and euthanized as soon as signs of morbidity became apparent. The median survival of control B-ALL recipient mice was 14 d, whereas the median survival of MyoIIA KD B-ALL recipient mice was 21.5 d (the 2 survival curves are statistically different, with $P < 0.0001$). (B–F) Progression of MyoIIA KD B-ALL leukemia is reduced compared with control B-ALL leukemia. Randomly selected leukemia recipient mice were euthanized, 3, 6, or 9 d post-transfer of 5×10^4 control or MyoIIA KD B-ALL cells. The frequency of B-ALL cells among the recovered live cells from each organ analyzed was quantified by flow cytometry. B-ALL cells were identified by ZsGreen and CD45.2 expression vs. endogenous leukocytes, which are CD45.1$^+$. $^{**}P < 0.01$, $^{***}P < 0.001$, $^{****}P < 0.0001$. (A) Data are pooled from 4 independent experiments with cohorts of 5 mice/group each. (B–F) Data are the means ± SEM of 4 independent experiments with 1 recipient mouse/group/time point.

2.5×10^6 differentially dye labeled control, and MyoIIA KD B-ALL cells were coinjected (at a 1:1 ratio) intravenously into CD45.1$^+$ recipient mice. At 8 and 24 h post-transfer, the recipient mice were euthanized, and the number and ratio of control and MyoIIA KD B-ALL cells in the blood, bone marrow, and spleen were determined by flow cytometry. Our results showed significantly reduced numbers of MyoIIA KD cells compared with control cells in the bone marrow and spleen, 24 h post-transfer (**Fig. 3**), and our data also trended toward a greater reduction of MyoIIA KD B-ALL cells in the bone marrow vs. the blood. These data suggest that MyoIIA KD B-ALL cells have a reduced capacity to engraft in vivo. A possible explanation for the reduced engraftment of MyoIIA-deficient B-ALL cells could be a result of a reduced ability to migrate into the bone marrow, which can support the survival and growth of leukemia cells [35].

Inhibition of MyoIIA impairs the ability of leukemia cells to infiltrate the brain

In leukemia patients, relapse involving the CNS is a relatively frequent and deleterious occurrence [4–6]; therefore, we analyzed if MyoIIA inhibition could reduce the ability of leukemia cells to infiltrate the brain in vivo. Having seen reduced numbers of MyoIIA KD B-ALL cells in the brain, 9 d following leukemia cell transfer (Fig. 2F), we examined B-ALL infiltration into the brain at short time points after transfer (≤24 h) to minimize possible confounding effects of in vivo differences in cell proliferation and survival between control and MyoIIA KD B-ALL cells. For these experiments, we intravenously transferred control or MyoIIA KD B-ALL cells into CD45.1$^+$ recipient mice and quantified the number of B-ALL cells that had infiltrated the brain 18 h later. To distinguish between leukemia cells that were simply arrested on the vasculature as opposed to cells that had actually infiltrated the brain parenchyma, we used an established vascular antibody-staining method [36, 37]. Just before euthanasia, the recipient mice were intravenously injected with anti-CD19-APC antibodies to label transferred B-ALL cells (which are CD45.2$^+$) as well as endogenous B cells (which are CD45.1$^+$) in the vasculature. After euthanasia, blood was harvested, and the

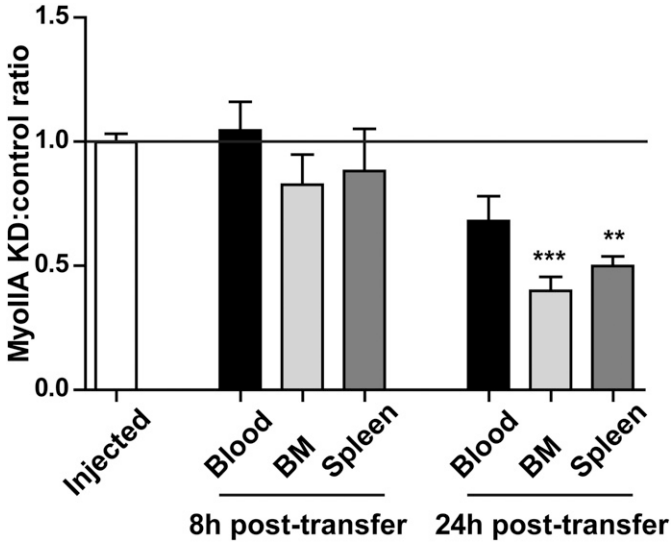

Figure 3. MyoIIA depletion reduces B-ALL cell engraftment. Leukemia engraftment is reduced in MyoIIA KD B-ALL cells. Differentially dye-labeled control and MyoIIA KD (shRNA 6592) B-ALL cells (2.5×10^6 each) were cotransferred at a 1:1 ratio by tail-vein injection into C57BL/6 CD45.1$^+$ mice. At 8 and 24 h post-transfer, the recipient mice were euthanized, and the number and ratio of control and MyoIIA KD B-ALL cells were determined in the blood, bone marrow (BM), and spleen by flow cytometry. B-ALL cells were identified by ZsGreen and CD45.2 expression vs endogenous leukocytes, which are CD45.1$^+$. A ratio below 1.0 (horizontal black line) indicates reduced numbers of MyoIIA KD cells. $^{**}P < 0.01$, $^{***}P < 0.001$ compared with the injected ratio.

recipient mice were perfused with saline to eliminate residual blood from tissues. The number of transferred leukemia cells was then quantified by flow cytometry analysis of single-cell suspensions obtained from the blood and brain using ZsGreen and CD45.2 as markers to discriminate the transferred B-ALL cells from endogenous cells. B-ALL cells recovered from the brain that were stained for CD19-APC were arrested in the vasculature, whereas CD19-APC-negative B-ALL cells from the brain had fully extravasated and entered the tissue (**Fig. 4A**). This analysis showed that MyoIIA KD B-ALL cells had a substantially reduced ability to infiltrate the brain compared with control cells. We found a significant increase in the percentage of MyoIIA-depleted cells arrested in the brain vasculature with a concomitant, drastic reduction of MyoIIA-depleted leukemia cells that had extravasated into the brain (Fig. 4B). Although the number of MyoIIA KD B-ALL cells was also reduced in the blood (the average ratio of control to MyoIIA KD B-ALL cells was ~2.5:1), the reduction was 5-fold greater in the brain (with an average ratio of ~12.5:1).

We confirmed further that MyoIIA promotes leukemia cell infiltration into the brain by use of the MyoII inhibitor

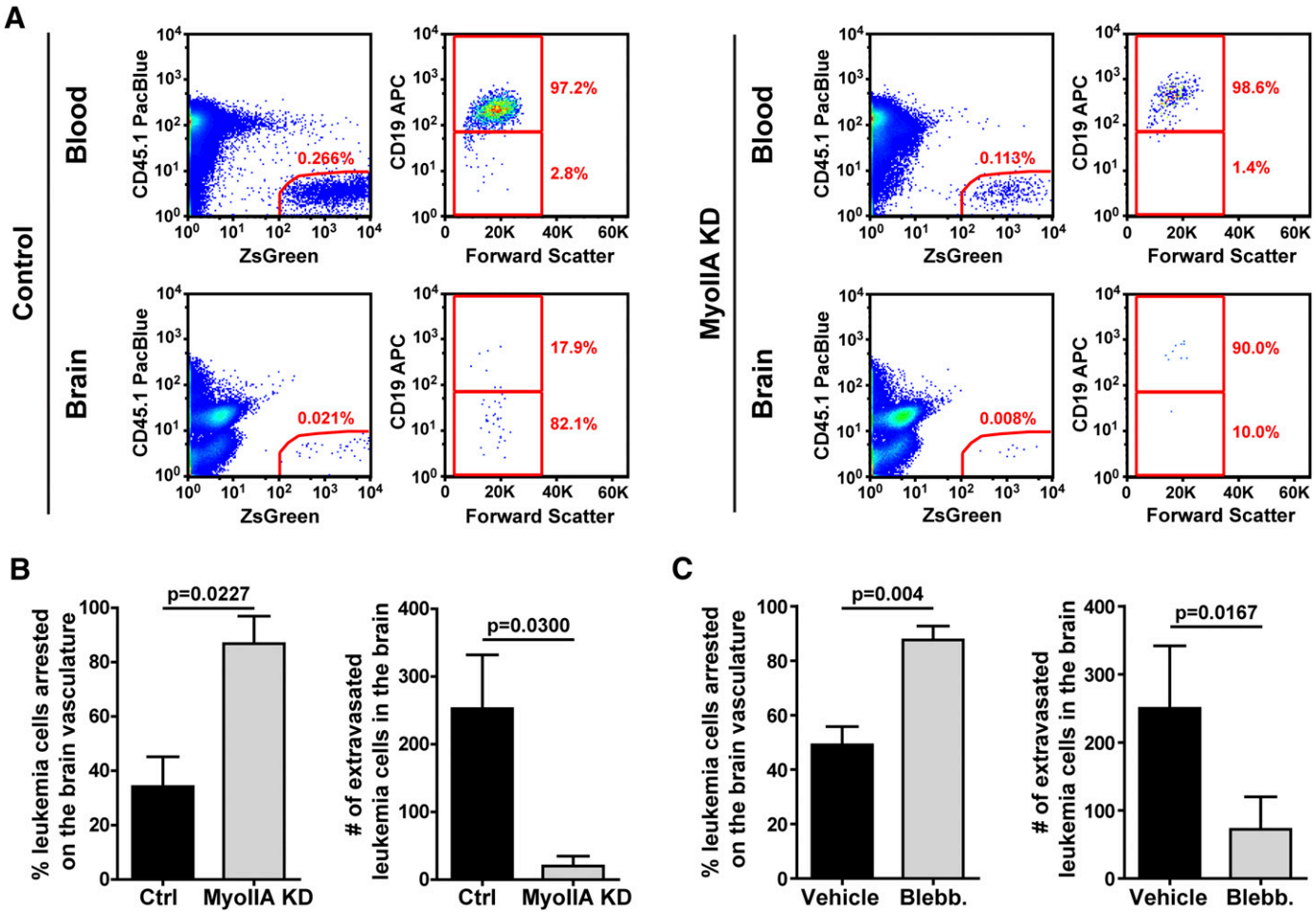

Figure 4. MyoIIA inhibition impairs the ability of B-ALL cells to extravasate in vivo and infiltrate the brain. ZsGreen$^+$ CD45.2$^+$ control or MyoIIA KD (shRNA 6592) B-ALL cells (2×10^7 each) were transferred intravenously into wild-type, congenically marked C57BL/6 CD45.1$^+$ recipient mice. Eighteen hours after transfer, to mark the transferred B-ALL cell present in the vasculature, the recipient mice were intravenously injected with CD19-APC antibodies and then euthanized 4 min later. B-ALL cells (ZsGreen$^+$ CD45.1$^-$), recovered from the brain that stained for CD19-APC, were considered to still be arrested in the vasculature, whereas CD19-APC-negative B-ALL cells recovered from the brain were considered as having fully extravasated and entered the brain parenchyma. (A) Representative flow cytometric analysis of B-ALL cell extravasation and infiltration into the brain. Live cells were gated by forward- and side-scatter and by a single-cell gate (not shown), and then transferred B-ALL cells were gated using a ZsGreen$^+$ CD45.1$^-$ gate (left). B-ALL cells that were arrested in the vasculature vs. cells that had fully infiltrated the brain were distinguished by CD19$^+$ or CD19$^-$ gates, respectively (right). (B) MyoIIA deficiency inhibits the capacity of B-ALL cells to complete extravasation in vivo. (Left) Frequency of control and MyoIIA KD B-ALL cells arrested in the brain vasculature that have not infiltrated the brain (ZsGreen$^+$ CD45.1$^-$ CD19$^+$). (Right) Quantification of the total number of control and MyoIIA KD B-ALL cells that fully extravasated and infiltrated the brain (ZsGreen$^+$ CD45.1$^-$ CD19$^-$). (C) MyoIIA inhibition by blebbistatin treatment in vivo impairs leukemia cell extravasation into the brain. One hour before B-ALL cell transfer, C57BL/6 CD45.1$^+$ recipient mice were treated with vehicle or blebbistatin (2.5 mg/kg). Twenty-four hours after B-ALL cell transfer, the recipient mice were intravenously injected with CD19-APC antibodies and then euthanized 4 min later. Data were analyzed as in B. (Left) Frequency of B-ALL cells arrested in the brain vasculature of vehicle or blebbistatin-treated mice. (Right) Quantification of the total number of B-ALL cells that fully infiltrated the brain of vehicle or blebbistatin-treated mice. (A) Data are representative of 4 independent experiments. (B and C) Data are the means ± SEM of 4 and 5 independent experiments, respectively.

blebbistatin [34] in vivo. We transferred equal numbers of control B-ALL cells into CD45.1$^+$ recipient mice that were intravenously treated with vehicle or blebbistatin, 1 h before B-ALL transfer. Twenty-four hours later, the number of B-ALL remaining stuck in the brain vasculature or having fully infiltrated the brain in vehicle vs. blebbistatin-treated recipient mice was quantified (as just described). Our results showed that with a very similar effect to MyoIIA KD, B-ALL cell infiltration into the brain was reduced significantly by in vivo blebbistatin treatment (Fig. 4C). This suggests that MyoIIA plays a key role in allowing leukemia cells to extravasate through the restrictive brain endothelial barrier and enter the brain.

TEM and chemotaxis are defective in MyoIIA-deficient leukemia cells

Having seen a strong effect of MyoIIA deficiency on the ability of B-ALL cells to infiltrate the CNS, as well as engraft in the bone marrow, we analyzed how MyoIIA inhibition affected B-ALL migration to investigate the mechanism of this impaired tissue infiltration. Pre-B cells, as well as many pre-B cell leukemia cells, respond to the chemokine CXCL12, which can play a role in their homing to the bone marrow niche [38, 39] and is expressed in the CNS. Therefore, we examined if MyoIIA deficiency impaired B-ALL cell chemotaxis toward CXCL12. With the use of a Transwell assay, we tested the migration of B-ALL cells through 5 μm pores in the absence or presence of CXCL12 in the bottom chamber. In the absence of CXCL12, there was almost no detectable B-ALL migration (<0.5% of the input). However, control B-ALL cells migrated robustly in response to CXCL12, and we found a significant reduction of CXCL12-mediated chemotaxis of MyoIIA KD B-ALL cells compared with shRNA control cells (**Fig. 5A**). With the use of the class II myosin inhibitor blebbistatin, we confirmed further the specificity of the effect of shRNA-mediated KD of MyoIIA in reducing CXCL12-mediated chemotaxis in B-ALL cells (Fig. 5A). The stronger reduction in chemotaxis by blebbistatin treatment is likely a result of the more complete drug-mediated, acute inhibition of MyoIIA, as opposed to the MyoIIA KD cells that still express ~15% residual MyoIIA protein. We then investigated whether reduced migration and dissemination of the MyoIIA KD B-ALL cells could be a result of altered expression of chemokine receptors and adhesion molecules. We compared the expression of CXCR4 (the receptor for CXCL12) and of various integrins that play a role in homing and extravasation into tissues, between control and MyoIIA KD cells. Our analysis found no major changes, ruling out differences in surface expression of CXCR4, CD11a, CD29, and CD49d as the main mechanism for impaired dissemination of MyoIIA KD B-ALL cells (Fig. 5B–E).

We next examined if, in addition to chemotaxis, TEM of B-ALL cells would be impaired by MyoIIA depletion as a further mechanism to explain the reduced extravasation of MyoIIA KD B-ALL cells in vivo. We used a system that we previously used to image lymphocyte TEM in real-time using confocal fluorescent and phase microscopy [15]. We analyzed B-ALL cell TEM under physiologic shear flow (2 dynes/cm^2) over a monolayer of brain-derived endothelial cells using time-lapse microscopy (**Fig. 6** and Supplemental Videos 1 and 2). We defined the position and

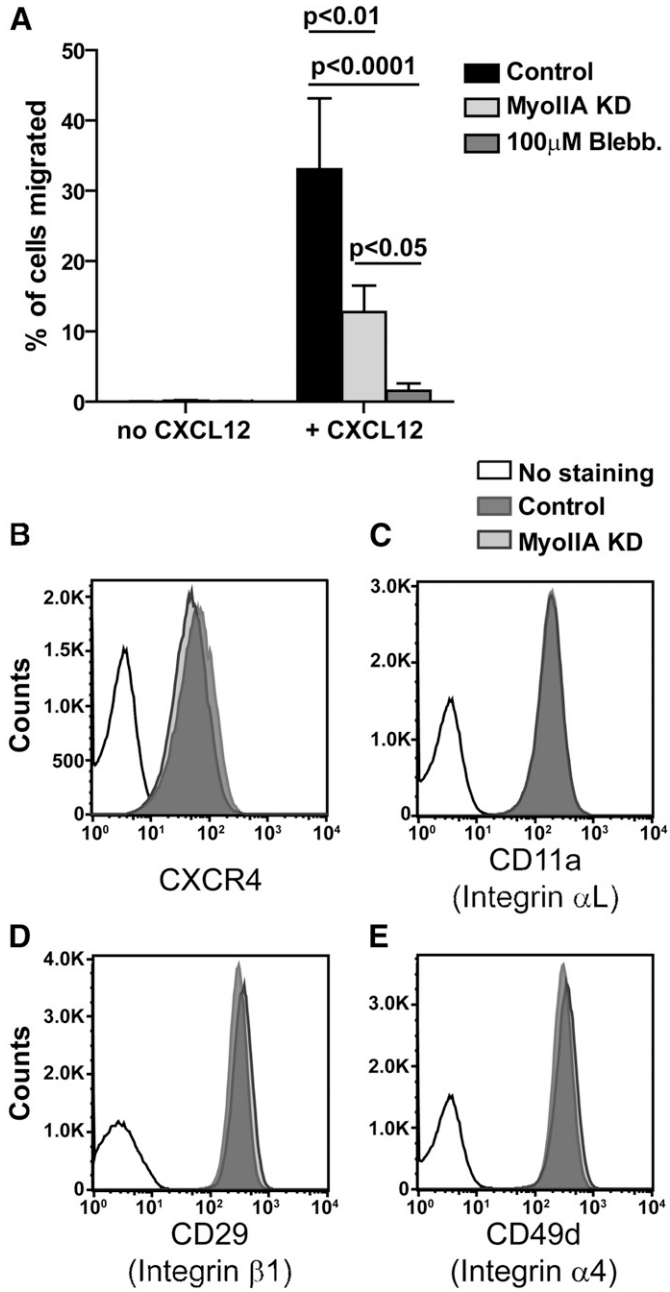

Figure 5. MyoIIA-inhibited B-ALL cells are defective in chemotaxis to CXCL12. (A) The percentage of chemotactic migration through 5 μm pore Transwells, with or without 1 μg/ml CXCL12 of control, MyoIIA KD (shRNA 6592), and blebbistatin-treated control B-ALL cells, was measured using flow cytometry in the presence of counting beads. (B–E) Control and MyoIIA KD B-ALL cells have similar surface expression of the chemokine receptor CXCR4 and of adhesion molecules. Control and MyoIIA KD B-ALL cells were stained for CXCR4 and the integrins CD11a, CD29, and CD49d, as indicated and analyzed by flow cytometry. (A) Data are the means ± SEM of 3 independent experiments. (B–E) Data are representative of 2 independent experiments.

migration of B-ALL cells relative to the endothelial cell monolayer using phase microscopy, in which B-ALL cells are surrounded by a white "phase ring" when above the endothelial cells and display a darkening of the phase ring when undergoing

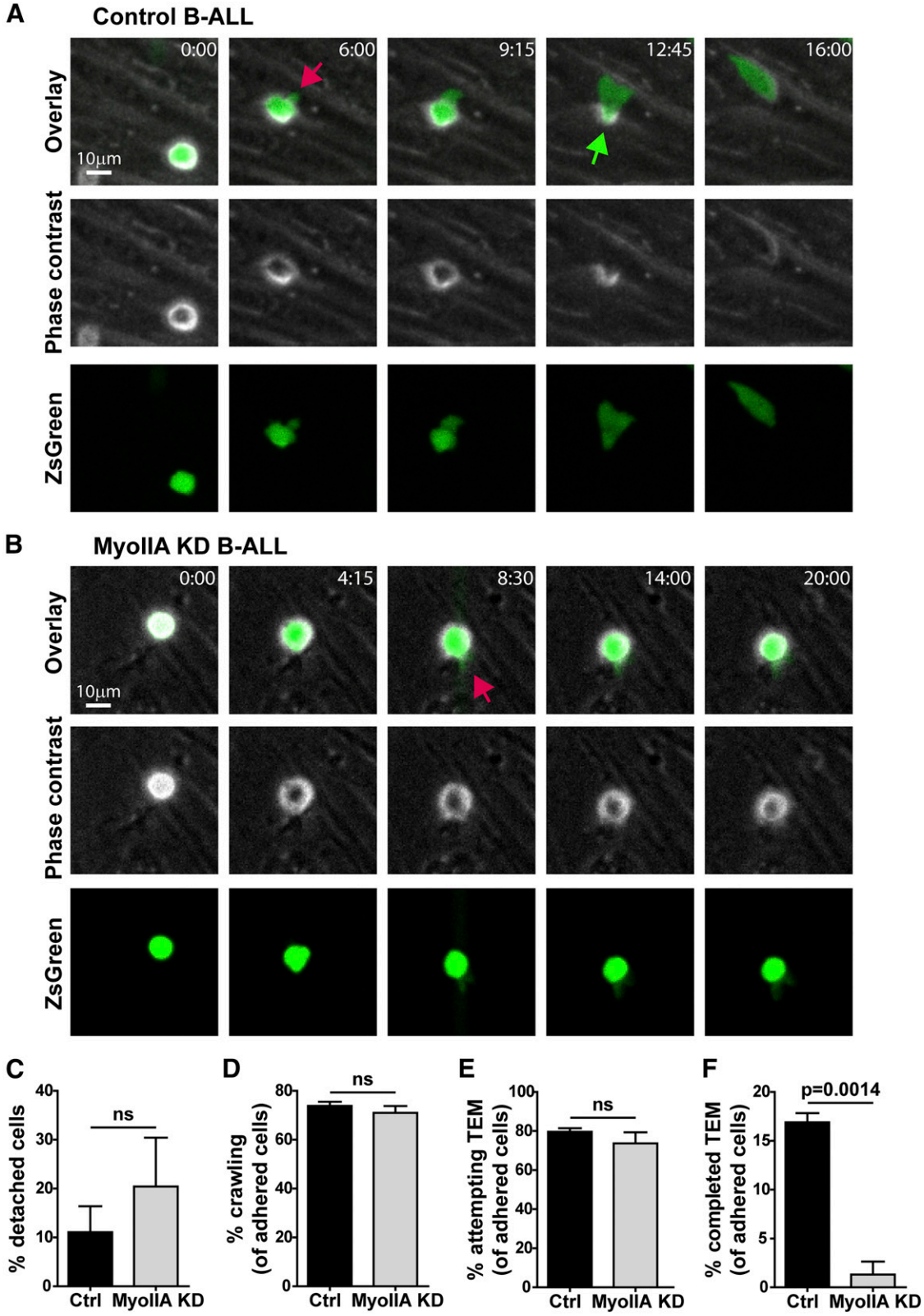

Figure 6. MyoIIA-deficient B-ALL cells are impaired in completing TEM. ZsGreen^{+} control or MyoIIA-depleted (shRNA 6592) B-ALL cells were perfused into flow chambers containing bEnd.3 brain endothelial cell monolayers and kept under shear flow (2 dyne/cm^2) for up to 30 min. During this time, phase contrast and green fluorescence images were acquired every 15 s using a spinning-disk confocal microscope. Time in minutes:seconds. (A) Selected time points of a representative control B-ALL cell during transmigration. This transmigrating leukemia cell undergoes

(*continued on next page*)

TEM through the endothelial cells (Fig. 6A). To confirm the integrity of endothelial monolayers and visualize endothelial junctions, before the addition of leukemia cells, the endothelial monolayers were stained with CD31 antibodies (not shown), which do not interfere with the TEM process [29, 30]. TEM attempts by B-ALL cells were determined by the opening of CD31-labeled endothelial junctions underneath leukemia cells. Completion of TEM was scored as full loss of the white phase ring, followed by crawling under the endothelial cells. Our results showed that of the B-ALL cells that adhered to the endothelial monolayer, control and MyoIIA KD B-ALL cells had comparable frequencies of the following: cell detachment from the endothelial monolayer (Fig. 6C), cells crawling over the endothelial monolayer (Fig. 6D), and cells attempting TEM (Fig. 6E). However, we found a dramatic reduction in the frequency of adhered MyoIIA KD B-ALL cells that were able to complete TEM compared with control cells (Fig. 6F). This indicates that the reduced entry of MyoIIA-deficient B-ALL cells into tissues in vivo is most likely a result of their impaired ability to extravasate through the endothelial blood vessel wall.

DISCUSSION

Whereas MyoIIA has been implicated in regulating lymphocyte migration [15, 16, 19, 20], as well as leukemia motility in vitro [25, 26], its role in lymphocytic leukemia TEM and in vivo dissemination has not been determined previously. In this study, we found that MyoIIA plays a key role in allowing B-ALL cells to undergo TEM and to extravasate into tissues in vivo.

Our results show that MyoIIA depletion impairs B-ALL cell chemotaxis and TEM. MyoIIA promotes lymphocyte TEM by providing the contractile force necessary to squeeze the rigid nucleus through small openings between endothelial cells and by detaching the back of the cell [15, 20]. Consistent with our previous findings that use activated T cells [15], MyoIIA-depleted leukemia cells, although able to initiate TEM, are severely deficient in their ability to complete the TEM process. Upstream of MyoIIA, the GTPase Rac can act as a negative regulator of MyoIIA activity by promoting phosphorylation of its heavy chains [40], which can lead to disassembly of MyoIIA complexes and inhibition of its contractile function [41]. Consistent with this role of Rac on MyoIIA activity and with our data on MyoIIA regulation of B-ALL TEM, Rac inhibition has been shown to increase leukemia cell migration in vitro in response to CXCL12 [42]. A further mechanism of action of MyoIIA in lymphocyte migration can be attributed to the association of MyoIIA with CXCR4, the receptor for CXCL12 [43], which may contribute to the transduction of chemotactic signals into force generation for migration. In T cells MyoIIA is involved in endocytosis of CXCR4 [44], it is therefore possible that depending on the circumstances, in addition to promoting chemotaxis toward CXCL12, MyoIIA can be part of a negative-feedback loop regulating chemotaxis through receptor endocytosis. However, our data suggest that MyoIIA depletion does not affect the steady-state expression of CXCR4 in B-ALL cells. Furthermore, MyoIIA has been shown to promote leukemia cell in vitro motility in response to CXCL12 [25], and our data that use B-ALL cells show that MyoIIA has a key role in mediating chemotaxis toward a CXCL12 gradient, which can mediate leukemia cell homing to the bone marrow as well as recruitment into the brain.

Our in vivo data show that MyoIIA-depleted leukemia cells have reduced ability to engraft upon transfer into recipient mice. This is likely a result of a migration defect that affects their capacity to home to the bone marrow and interact with bone marrow stromal cells, which can support the survival and growth of leukemia cells [35]. Leukemia cells rely on CXCR4 signaling for homing and engraftment in the bone marrow [45–47], and MyoIIA deficiency can affect bone marrow homing of leukemia cells by interfering with CXCR4-dependent chemotaxis and the mechanical ability of leukemia cells to extravasate. This reduced bone marrow homing of the MyoIIA KD B-ALL cells may therefore lead to reduced survival of the transferred leukemia cells and their slower growth rate in vivo.

Finally, we have shown that impaired TEM, through brain endothelial cells of MyoIIA-deficient leukemia cells, results in a significantly reduced capacity to infiltrate into the brain. With the use of the MyoII inhibitor blebbistatin in vivo, we have confirmed, through a second independent mode of interfering with MyoIIA function, a strong requirement for MyoIIA in allowing leukemia cells to infiltrate the brain. This effect of MyoIIA inhibition could be of important clinical relevance as a result of the fact that leukemia cells that enter the CNS are a frequent cause of relapse [6, 48, 49]. Our data that use blebbistatin to prevent B-ALL infiltration into the brain also suggest that this MyoII inhibitor has efficacy in vivo and that MyoIIA may be a druggable target for clinical applications. Future work will further determine the feasibility and safety of using blebbistatin in vivo, particularly over prolonged periods of time in the context of leukemia.

In conclusion, we report that MyoIIA regulates B-ALL cell migration, engraftment, and infiltration into the brain and that MyoIIA depletion prolongs survival in a mouse model of B-ALL. Overall, these findings suggest that MyoIIA could be an attractive target for the treatment of B-ALL, particularly as various signaling pathways, which may be altered in transformed lymphocytes, converge on MyoIIA to promote

TEM, evidenced by a step-wise darkening in the phase-contrast channel during the time lapse. The red arrow points to the formation of membrane protrusions under the endothelial monolayer; the green arrow points to the cell completing TEM, as shown by the disappearance of the phase ring. (B) Selected time points of a representative MyoIIA KD B-ALL cell attempting transmigration. The red arrow points to the formation of membrane protrusions under the endothelial monolayer; however, this MyoIIA KD cell never completes TEM, as evidenced by the preservation of the phase ring. (C–F) Of the B-ALL cells that adhered to the endothelial monolayer for at least 5 min, the percentage of B-ALL cells that detached, crawled over the endothelial cells, attempted TEM (evidenced by extension of membrane protrusions underneath the endothelial monolayer), and completed TEM was calculated. (C) MyoIIA KD does not significantly affect leukemia cell detachment from the endothelial cell monolayer. (D) Control and MyoIIA KD B-ALL cells have similar crawling over the endothelial monolayer. (E) MyoIIA KD does not affect the ability of B-ALL cells to attempt TEM. (F) MyoIIA depletion significantly impairs the ability of B-ALL leukemia to complete TEM. (A and B) Data are representative of 3 independent experiments. (C–F) Data are the means ± SEM of 3 independent experiments.

migration. Specifically, in combination with existing therapies, such as TKIs and chemotherapy, MyoIIA inhibition can impair homing of leukemia cells to the bone marrow, as well as infiltration into the brain, with both organs being environments in which leukemia cells can find protection from treatments [4, 49, 50]. Therefore, MyoIIA inhibition could potentially synergize with other anti-leukemia treatments to eradicate leukemia cells more completely, while at the same time preventing relapses.

AUTHORSHIP

E.J.W. and S.B.T. performed the experiments and participated in designing some experiments. R.A.L. participated in the cloning of the shRNA constructs and in performing some of the in vivo experiments. E.J.W., S.B.T., and J.J. analyzed and interpreted the data and created figures. S.B.T. and J.J. wrote the manuscript. J.J. conceived of and designed the experiments and supervised the overall project.

ACKNOWLEDGMENTS

This work was supported, in part, by the Wendy Siegel Fund for Leukemia and Cancer Research, Cancer League of Colorado, and Driskill Foundation (all to J.J.). This work was also supported, in part, by the University of Colorado Cancer Center's Flow Cytometry Shared Resource, funded by the U. S. National Institutes of Health National Cancer Institute Support Grant P30-CA046934. The authors thank M. Gebert, B. Traxinger, and M. Fisher for help with mouse genotyping and colony maintenance; M. Fisher and R. Lindsay for technical help with some experiments; J. Loomis and S. Sobus for expert technical assistance with cell sorting; and J. Loomis for microscope maintenance. The authors also thank Drs. J. DeGregori and R. Friedman for feedback, reagents, and critical reading of the manuscript.

DISCLOSURES

The authors declare no conflicts of interest.

REFERENCES

1. Yeoh, E. J., Ross, M. E., Shurtleff, S. A., Williams, W. K., Patel, D., Mahfouz, R., Behm, F. G., Raimondi, S. C., Relling, M. V., Patel, A., Cheng, C., Campana, D., Wilkins, D., Zhou, X., Li, J., Liu, H., Pui, C. H., Evans, W. E., Naeve, C., Wong, L., Downing, J. R. (2002) Classification, subtype discovery, and prediction of outcome in pediatric acute lymphoblastic leukemia by gene expression profiling. *Cancer Cell* **1,** 133–143.
2. Pfeifer, H., Wassmann, B., Hofmann, W. K., Komor, M., Scheuring, U., Bruck, P., Binckebanck, A., Schleyer, E., Gokbuget, N., Wolff, T., Lubbert, M., Leimer, L., Gschaidmeier, H., Hoelzer, D., Ottmann, O. G. (2003) Risk and prognosis of central nervous system leukemia in patients with Philadelphia chromosome-positive acute leukemias treated with imatinib mesylate. *Clin. Cancer Res.* **9,** 4674–4681.
3. Leis, J. F., Stepan, D. E., Curtin, P. T., Ford, J. M., Peng, B., Schubach, S., Druker, B. J., Maziarz, R. T. (2004) Central nervous system failure in patients with chronic myelogenous leukemia lymphoid blast crisis and Philadelphia chromosome positive acute lymphoblastic leukemia treated with imatinib (STI-571). *Leuk. Lymphoma* **45,** 695–698.
4. Aragon-Ching, J. B., Zujewski, J. A. (2007) CNS metastasis: an old problem in a new guise. *Clin. Cancer Res.* **13,** 1644–1647.
5. Wolff, N. C., Richardson, J. A., Egorin, M., Ilaria, Jr., R. L. (2003) The CNS is a sanctuary for leukemic cells in mice receiving imatinib mesylate for Bcr/Abl-induced leukemia. *Blood* **101,** 5010–5013.
6. Pui, C.-H., Howard, S. C. (2008) Current management and challenges of malignant disease in the CNS in paediatric leukaemia. *Lancet Oncol.* **9,** 257–268.
7. Nguyen, K., Devidas, M., Cheng, S. C., La, M., Raetz, E. A., Carroll, W. L., Winick, N. J., Hunger, S. P., Gaynon, P. S., Loh, M. L. (2008) Factors influencing survival after relapse from acute lymphoblastic leukemia: a Children's Oncology Group study. *Leukemia* **22,** 2142–2150.
8. Arbonés, M. L., Ord, D. C., Ley, K., Ratech, H., Maynard-Curry, C., Otten, G., Capon, D. J., Tedder, T. F. (1994) Lymphocyte homing and leukocyte rolling and migration are impaired in L-selectin-deficient mice. *Immunity* **1,** 247–260.
9. Campbell, J. J., Hedrick, J., Zlotnik, A., Siani, M. A., Thompson, D. A., Butcher, E. C. (1998) Chemokines and the arrest of lymphocytes rolling under flow conditions. *Science* **279,** 381–384.
10. Ley, K., Laudanna, C., Cybulsky, M. I., Nourshargh, S. (2007) Getting to the site of inflammation: the leukocyte adhesion cascade updated. *Nat. Rev. Immunol.* **7,** 678–689.
11. Nourshargh, S., Hordijk, P. L., Sixt, M. (2010) Breaching multiple barriers: leukocyte motility through venular walls and the interstitium. *Nat. Rev. Mol. Cell Biol.* **11,** 366–378.
12. Krummel, M. F., Friedman, R. S., Jacobelli, J. (2014) Modes and mechanisms of T cell motility: roles for confinement and myosin-IIA. *Curr. Opin. Cell Biol.* **30,** 9–16.
13. Pals, S. T., de Gorter, D. J., Spaargaren, M. (2007) Lymphoma dissemination: the other face of lymphocyte homing. *Blood* **110,** 3102–3111.
14. Meacham, C. E., Ho, E. E., Dubrovsky, E., Gertler, F. B., Hemann, M. T. (2009) In vivo RNAi screening identifies regulators of actin dynamics as key determinants of lymphoma progression. *Nat. Genet.* **41,** 1133–1137.
15. Jacobelli, J., Estin Matthews, M., Chen, S., Krummel, M. F. (2013) Activated T cell trans-endothelial migration relies on myosin-IIA contractility for squeezing the cell nucleus through endothelial cell barriers. *PLoS One* **8,** e75151.
16. Jacobelli, J., Friedman, R. S., Conti, M. A., Lennon-Dumenil, A. M., Piel, M., Sorensen, C. M., Adelstein, R. S., Krummel, M. F. (2010) Confinement-optimized three-dimensional T cell amoeboid motility is modulated via myosin IIA-regulated adhesions. *Nat. Immunol.* **11,** 953–961.
17. Conti, M. A., Adelstein, R. S. (2008) Nonmuscle myosin II moves in new directions. *J. Cell Sci.* **121,** 11–18.
18. Vicente-Manzanares, M., Ma, X., Adelstein, R. S., Horwitz, A. R. (2009) Non-muscle myosin II takes centre stage in cell adhesion and migration. *Nat. Rev. Mol. Cell Biol.* **10,** 778–790.
19. Morin, N. A., Oakes, P. W., Hyun, Y. M., Lee, D., Chin, Y. E., King, M. R., Springer, T. A., Shimaoka, M., Tang, J. X., Reichner, J. S., Kim, M. (2008) Nonmuscle myosin heavy chain IIA mediates integrin LFA-1 de-adhesion during T lymphocyte migration. *J. Exp. Med.* **205,** 195–205.
20. Soriano, S. F., Hons, M., Schumann, K., Kumar, V., Dennier, T. J., Lyck, R., Sixt, M., Stein, J. V. (2011) In vivo analysis of uropod function during physiological T cell trafficking. *J. Immunol.* **187,** 2356–2364.
21. Dulyaninova, N. G., House, R. P., Betapudi, V., Bresnick, A. R. (2007) Myosin-IIA heavy-chain phosphorylation regulates the motility of MDA-MB-231 carcinoma cells. *Mol. Biol. Cell* **18,** 3144–3155.
22. Ivkovic, S., Beadle, C., Noticewala, S., Massey, S. C., Swanson, K. R., Toro, L. N., Bresnick, A. R., Canoll, P., Rosenfeld, S. S. (2012) Direct inhibition of myosin II effectively blocks glioma invasion in the presence of multiple motogens. *Mol. Biol. Cell* **23,** 533–542.
23. Beach, J. R., Hussey, G. S., Miller, T. E., Chaudhury, A., Patel, P., Monslow, J., Zheng, Q., Keri, R. A., Reizes, O., Bresnick, A. R., Howe, P. H., Egelhoff, T. T. (2011) Myosin II isoform switching mediates invasiveness after TGF-β-induced epithelial-mesenchymal transition. *Proc. Natl. Acad. Sci. USA* **108,** 17991–17996.
24. Li, Z. H., Bresnick, A. R. (2006) The S100A4 metastasis factor regulates cellular motility via a direct interaction with myosin-IIA. *Cancer Res.* **66,** 5173–5180.
25. Jbireal, J., Dittmar, T., Niggemann, B., Fischer, J., Entschladen, F. (2012) Differential involvement of myosin II and VI in the spontaneous and SDF 1-induced migration of adult CD133+ hematopoietic stem/progenitor cells and leukemic cells. *Curr. Cancer Ther. Rev.* **8,** 283–292.
26. Jbireal, J. M., Strell, C., Niggemann, B., Zänker, K., Entschladen, F. (2010) The selective role of myosin VI in lymphoid leukemia cell migration. *Leuk. Res.* **34,** 1656–1662.
27. Williams, R. T., Roussel, M. F., Sherr, C. J. (2006) Arf gene loss enhances oncogenicity and limits imatinib response in mouse models of Bcr-Abl-induced acute lymphoblastic leukemia. *Proc. Natl. Acad. Sci. USA* **103,** 6688–6693.
28. Jacobelli, J., Bennett, F. C., Pandurangi, P., Tooley, A. J., Krummel, M. F. (2009) Myosin-IIA and ICAM-1 regulate the interchange between two distinct modes of T cell migration. *J. Immunol.* **182,** 2041–2050.
29. Christofidou-Solomidou, M., Nakada, M. T., Williams, J., Muller, W. A., DeLisser, H. M. (1997) Neutrophil platelet endothelial cell adhesion molecule-1 participates in neutrophil recruitment at inflammatory sites and is down-regulated after leukocyte extravasation. *J. Immunol.* **158,** 4872–4878.
30. Woodfin, A., Voisin, M. B., Beyrau, M., Colom, B., Caille, D., Diapouli, F. M., Nash, G. B., Chavakis, T., Albelda, S. M., Rainger, G. E., Meda, P., Imhof,

B. A., Nourshargh, S. (2011) The junctional adhesion molecule JAM-C regulates polarized transendothelial migration of neutrophils in vivo. *Nat. Immunol.* **12,** 761–769.
31. Boulos, N., Mulder, H. L., Calabrese, C. R., Morrison, J. B., Rehg, J. E., Relling, M. V., Sherr, C. J., Williams, R. T. (2011) Chemotherapeutic agents circumvent emergence of dasatinib-resistant BCR-ABL kinase mutations in a precise mouse model of Philadelphia chromosome-positive acute lymphoblastic leukemia. *Blood* **117,** 3585–3595.
32. Williams, R. T., den Besten, W., Sherr, C. J. (2007) Cytokine-dependent imatinib resistance in mouse BCR-ABL+, Arf-null lymphoblastic leukemia. *Genes Dev.* **21,** 2283–2287.
33. Jacobelli, J., Chmura, S. A., Buxton, D. B., Davis, M. M., Krummel, M. F. (2004) A single class II myosin modulates T cell motility and stopping, but not synapse formation. *Nat. Immunol.* **5,** 531–538.
34. Straight, A. F., Cheung, A., Limouze, J., Chen, I., Westwood, N. J., Sellers, J. R., Mitchison, T. J. (2003) Dissecting temporal and spatial control of cytokinesis with a myosin II inhibitor. *Science* **299,** 1743–1747.
35. Burger, M., Hartmann, T., Krome, M., Rawluk, J., Tamamura, H., Fujii, N., Kipps, T. J., Burger, J. A. (2005) Small peptide inhibitors of the CXCR4 chemokine receptor (CD184) antagonize the activation, migration, and antiapoptotic responses of CXCL12 in chronic lymphocytic leukemia B cells. *Blood* **106,** 1824–1830.
36. Anderson, K. G., Mayer-Barber, K., Sung, H., Beura, L., James, B. R., Taylor, J. J., Qunaj, L., Griffith, T. S., Vezys, V., Barber, D. L., Masopust, D. (2014) Intravascular staining for discrimination of vascular and tissue leukocytes. *Nat. Protoc.* **9,** 209–222.
37. Pereira, J. P., An, J., Xu, Y., Huang, Y., Cyster, J. G. (2009) Cannabinoid receptor 2 mediates the retention of immature B cells in bone marrow sinusoids. *Nat. Immunol.* **10,** 403–411.
38. Burger, J. A., Peled, A. (2009) CXCR4 antagonists: targeting the microenvironment in leukemia and other cancers. *Leukemia* **23,** 43–52.
39. Tavor, S., Petit, I. (2010) Can inhibition of the SDF-1/CXCR4 axis eradicate acute leukemia? *Semin. Cancer Biol.* **20,** 178–185.
40. Van Leeuwen, F. N., van Delft, S., Kain, H. E., van der Kammen, R. A., Collard, J. G. (1999) Rac regulates phosphorylation of the myosin-II heavy chain, actinomyosin disassembly and cell spreading. *Nat. Cell Biol.* **1,** 242–248.
41. Dulyaninova, N. G., Malashkevich, V. N., Almo, S. C., Bresnick, A. R. (2005) Regulation of myosin-IIA assembly and Mts1 binding by heavy chain phosphorylation. *Biochemistry* **44,** 6867–6876.
42. Freret, M., Gouel, F., Buquet, C., Legrand, E., Vannier, J. P., Vasse, M., Dubus, I. (2011) Rac-1 GTPase controls the capacity of human leukaemic lymphoblasts to migrate on fibronectin in response to SDF-1α (CXCL12). *Leuk. Res.* **35,** 971–973.
43. Rey, M., Vicente-Manzanares, M., Viedma, F., Yáñez-Mó, M., Urzainqui, A., Barreiro, O., Vázquez, J., Sánchez-Madrid, F. (2002) Cutting edge: association of the motor protein nonmuscle myosin heavy chain-IIA with the C terminus of the chemokine receptor CXCR4 in T lymphocytes. *J. Immunol.* **169,** 5410–5414.
44. Rey, M., Valenzuela-Fernández, A., Urzainqui, A., Yáñez-Mó, M., Pérez-Martínez, M., Penela, P., Mayor, Jr., F., Sánchez-Madrid, F. (2007) Myosin IIA is involved in the endocytosis of CXCR4 induced by SDF-1alpha. *J. Cell Sci.* **120,** 1126–1133.
45. Sipkins, D. A., Wei, X., Wu, J. W., Runnels, J. M., Côté, D., Means, T. K., Luster, A. D., Scadden, D. T., Lin, C. P. (2005) In vivo imaging of specialized bone marrow endothelial microdomains for tumour engraftment. *Nature* **435,** 969–973.
46. Spiegel, A., Kollet, O., Peled, A., Abel, L., Nagler, A., Bielorai, B., Rechavi, G., Vormoor, J., Lapidot, T. (2004) Unique SDF-1-induced activation of human precursor-B ALL cells as a result of altered CXCR4 expression and signaling. *Blood* **103,** 2900–2907.
47. Shen, W., Bendall, L. J., Gottlieb, D. J., Bradstock, K. F. (2001) The chemokine receptor CXCR4 enhances integrin-mediated in vitro adhesion and facilitates engraftment of leukemic precursor-B cells in the bone marrow. *Exp. Hematol.* **29,** 1439–1447.
48. Jabbour, E., Thomas, D., Cortes, J., Kantarjian, H. M., O'Brien, S. (2010) Central nervous system prophylaxis in adults with acute lymphoblastic leukemia: current and emerging therapies. *Cancer* **116,** 2290–2300.
49. Barredo, J., Ritchey, A. K. (2010) Controversies in the management of central nervous system leukemia. *Pediatr. Hematol. Oncol.* **27,** 329–332.
50. Manabe, A., Murti, K. G., Coustan-Smith, E., Kumagai, M., Behm, F. G., Raimondi, S. C., Campana, D. (1994) Adhesion-dependent survival of normal and leukemic human B lymphoblasts on bone marrow stromal cells. *Blood* **83,** 758–766.

KEY WORDS:
cytoskeleton · migration · extravasation · dissemination · Bcr-Abl